Dynamical effects of loss of cooperation in discrete-time hypercycles

Júlia Perona,[1] Ernest Fontich,[1,2,*] and Josep Sardanyés[3,2,†]

[1] *Departament de Matemàtiques i Informàtica, Gran Via 585, 08007 Barcelona. Universitat de Barcelona (UB), Spain*
[2] *Barcelona Graduate School of Mathematics (BGSMath), Campus de Bellaterra, Edifici C, 08193 Bellaterra, Spain*
[3] *Centre de Recerca Matemàtica (CRM), Campus de Bellaterra, Edifici C, 08193 Bellaterra, Spain*

Hypercycles' dynamics have been widely investigated in the context of origins of life, especially using time-continuous dynamical models. Different hypercycle architectures jeopardising their stability and persistence have been discussed and investigated, namely the catalytic parasites and the short-circuits. Here we address a different scenario considering RNA-based hypercycles in which cooperation is lost and catalysis shifts to density-dependent degradation processes due to the acquisition of cleaving activity by one hypercycle species. That is, we study the dynamical changes introduced by a functional shift. To do so we use a discrete-time model that can be approached to the time continuous limit by means of a temporal discretisation parameter, labelled C. We explore dynamical changes tied to the loss of cooperation in two-, three-, and four-member hypercycles in this discrete-time setting. With cooperation, the all-species coexistence in two- and three-member hypercycles is governed by an internal stable fixed point. When one species shifts to directed degradation, a transcritical bifurcation takes place and the other hypercycle members go to extinction. The asymptotic dynamics of the four-member system is governed by an invariant curve in its cooperative regime. For this system, we have identified a simultaneous degenerate transcritical–Neimark-Sacker bifurcation as cooperation switches to directed degradation. After these bifurcations, as we found for the other systems, all the cooperative species except the one performing degradation become extinct. Finally, we also found that the observed bifurcations and asymptotic dynamical behaviours are independent of C. Our results can help in understanding the impact of changes in ecological interactions (i.e., functional shifts) in multi-species systems and to determine the nature of the transitions tied to co-extinctions and out-competition processes in both ecosystems and RNA-based systems.

Keywords: Bifurcations, Discrete-time hypercycles, Functional shifts, Origins of Life, Nonlinear dynamics, Theoretical ecology

* corresponding author. E-mail: fontich@ub.edu
† corresponding author. E-mail: jsardanyes@crm.cat

I. INTRODUCTION

Hypercycles [1] are nonlinear dynamical systems formed by n polynucleotides with catalytic activity. Hypercycles have been mainly studied within the framework of prebiotic evolution and origins of life, providing a potential solution to the so-called prebiotic information crisis [1–3, 5]. The generality of hypercycle (replicator) equations has also allowed to employ this model in neural networks [6, 7], virus replication [8–10, 12], immune system [13], or ecosystem dynamics [5, 18], among others. Also, parallelisms about the error threshold and hypercycles have been discussed within the framework of the emergence of language [19]. Interestingly, hypercycles have been experimentally built using coiled-coil peptides [20], yeast cell populations [21], and cooperative engineered bacteria growing with catalytic parasites [22].

It has been argued that hypercycle species may need two minimal conditions in order to be evolutionary stable [3, 4], namely: (i) catalytic replication and (ii) capability of information storage. These two properties are found simultaneously in RNA-based replicons such as ribozymes (ribonucleic acid enzymes). RNAs with loop and stem structures, similar to those of modern tRNAs [23], are known to be stable against hydrolysis [24] also having replicability potential [25, 26]. Indeed, smaller functional RNAs have been found in viroids [27] and other RNAs [28]. Ribozymes are short RNA molecules able to catalyse specific biochemical reactions, similar to the action of protein enzymes [26, 29]. Hence, ribozymes have been considered as potential candidates forming the first autonomous, self-replicating molecular systems involved in the origins of life [3, 4, 25, 30–33]. Some of these hypothetic prebiotic RNAs were supposed to participate in ribosome-free translation of an appropriate messenger [31, 34].

Different activities have been described for natural and *in vitro* (e.g., peptide-bond formation [35]) evolved ribozymes. Certain introns can catalyse their own excision (self-cleavage) from single-stranded RNA (ssRNA) [26] and ligase reactions by RNA catalysts can occur even with short RNA sequences [36]. Moreover, the same RNA sequences can catalyse trans-esterification reactions for elongation of one monomer [26], ligation of two independent ssRNAs [37, 38], and cleavage of RNA into smaller sequences [26–28, 39] (see [31, 40] for reviews).

Despite the functional properties of ribozymes, RNA-catalysed self-replication from RNA templates seems to be quite limited. However, recent experiments evolving catalysts at sub-zero temperatures have revealed that the combination of RNAs with cold-adaptative mutations with a previously described $5'$ extension operating at ambient temperatures enabled catalysing the synthesis of an RNA sequence longer than itself (adding up to 206 nucleotides) [41]. Moreover, recent experiments have shown the spontaneous formation of catalytic cycles and networks from mixtures of RNA fragments able to self-assemble into self-replicating ribozymes [42], providing evidences for selective advantage of cooperative systems composed by ribozymes.

From the modelling point of view, hypercycles have been mainly investigated with continuous time approaches, for both well-mixed i.e., ordinary differential equations (ODEs) [1, 43–46, 48] and spatially-resolved [49, 51, 52] systems. ODEs typically reveal that the asymptotic coexistence for hypercycles with $n = 2, 3, 4$ species is typically governed by an interior stable equilibrium [1, 46, 53]. More specifically, the case $n = 2$ has a stable node [46], while cases $n = 3$ and $n = 4$ are governed by stable foci with fast and hardly damped oscillations [1, 45, 53], respectively. Moreover, a multitude of analyses (both numerical and analytical) have revealed that for $n > 4$, populations undergo self-sustained oscillations in its cooperative regime [1, 43, 44, 54]. To date, very few works have investigated hypercycles considering discrete time (e.g., using difference equations or maps [55, 56]), being mainly analysed with cellular automata models [47, 48, 50]. Specifically, the system studied by Hofbauer and others [55, 56] revealed that discrete-time hypercycles with $n = 2, 3$ have an interior stable fixed point governing coexistence dynamics, while the case $n = 4$ involves oscillating coexistence governed by an invariant curve.

In this article we consider the discrete hypercycle model developed in [55] to investigate the impact on the dynamics and the bifurcations when one of the species shifts from cooperative to antagonistic interactions. By the cyclic character of the system we can assume the species that shifts is the first one. To date, different architectural changes having a negative impact on hypercycles have been thoroughly investigated. These include the so-called catalytic parasites [47–49, 52] and short-circuits [50, 51], suggested to impair hypercycle's stability thus constraining the increase of information. The case we investigate in this article is different since the cyclic structure of the hypercycle is maintained but a given replicator instructs the degradation of the next species of the system, instead of providing catalytic aid. This new system is inspired in the existence of ribozymes with trans-cleaving functions. For example, minimal trans-cleaving RNA hammerheads were generated several decades ago [57, 58]. Also, both *in vitro* and *in vivo* hammerhead ribozymes with trans-cleaving activity against viroids have been described more recently [39].

As mentioned, we are interested in the dynamics when a given species shifts from cooperative to antagonistic interactions i.e., density-dependent degradation, focusing on small hypercycles with $n = 2, 3, 4$ species. Although we are not modelling this functional shift explicitly by considering mutations in the catalytic motifs and their change to cleaving motifs, we investigate this shift by taking a replication constant both either positive (catalysis) or negative (cleavage). The paper is organised as follows. In Section II we introduce the studied model [55], showing its relation with the ODEs model as the discretisation time parameter $C \to \infty$. Then, we compute the fixed points and the

eigenvalues for the general model in Section III A. In Section III B we analytically prove that, for any number of species, when the first species shifts to directed degradation, the asymptotic behaviour is a fixed point in the corner of the phase space, involving the out-competition of all other species providing catalytic aid. In Section III C we investigate the dynamics for the studied hypercycles with $n = 2, 3, 4$ species. In particular, we analytically determine the basin of attraction in the domain of the system. In Section III D we analytically obtain the rates of convergence for those cases where the $\omega-$limit is a fixed point, showing the relevant parameters in the asymptotic expression. Numerical computations confirm the analytic findings, in particular, we illustrate the linear dependence of the number of iterations to the fixed points with the parameter C. Finally, in Section III E we provide a numerical study of the invariant curves found for the case $n = 4$ and $k_i > 0$. The bifurcations tied to the functional shifts are also discussed in Sections III C and III E. Finally, Section IV is devoted to final conclusions.

II. MATHEMATICAL MODEL

In this section we introduce the discrete-time hypercycle model proposed by Hofbauer [55], that will be employed in this work to determine the impact of functional shifts in hypercycles. Let x_i denote the concentration of the i-th species, S_i, and k_i the kinetic constants that quantify the strength of catalysis that the $i-1$ species provides to the i-th species. For notational convenience the subindices i are modulo n, i.e., $x_0 = x_n$ and also $x_{n+1} = x_1$. The system is determined by an n-dimensional function $F : \mathbb{R}^n \to \mathbb{R}^n$, $F_i(x)$ being the concentration x_i in the next generation, i.e., $F_i(x)$ represents the concentration after one unit of time. This function considers replication rate of S_i to be proportional to the amount of S_{i-1}, according to the product $x_i\, x_{i-1}$ (catalytically-assisted replication), taking into account that the $(i-1)$-th species contributes to the replication of i-th one. We write

$$F_i(x) \sim x_i(C + k_i x_{i-1}), \qquad C > 0.$$

Next, we determine the proportionality factor $A(x)$ imposing the total population to be a constant. So if $\sum_{i=1}^n x_i = 1$ we want $\sum_{i=1}^n F_i(x) = 1$. This means

$$\sum_{i=1}^{n} A(x)x_i(C + k_i x_{i-1}) = A(x)\left(C + \sum_{i=1}^{n} k_i x_i x_{i-1}\right) = 1.$$

We introduce

$$\phi(x) = \sum_{i=1}^{n} k_i x_i x_{i-1}$$

and then $A(x)$ has to be equal to $(C + \phi(x))^{-1}$. Therefore, we have the following discrete-time system:

$$F_i(x) = \frac{C + k_i x_{i-1}}{C + \phi(x)} x_i, \qquad 1 \le i \le n. \tag{1}$$

The dynamics of Map (1) spans the following $(n-1)$-simplex:

$$S^{n-1} = \Big\{ x = (x_1, ..., x_n) \in \mathbb{R}^n \mid \sum_{i=1}^{n} x_i = 1 \text{ and } x_i \ge 0 \ \text{ for } i = 1, \cdots, n \Big\}.$$

To compare this map with an analogous continuous time model we rewrite the i-th component of F as follows:

$$F_i(x) - x_i = \frac{C + k_i x_{i-1}}{C + \phi(x)} x_i - x_i = \frac{k_i x_{i-1} - \phi(x)}{C + \phi(x)} x_i$$

so that

$$\frac{F_i(x) - x_i}{C^{-1}} = x_i(k_i x_{i-1} - \phi(x)) \frac{C}{C + \phi(x)}.$$

Interpreting now C^{-1} as the time interval between two generations, the Map (1) can be seen as the Euler C^{-1} step of the differential equation

$$\dot{x}_i = x_i(k_i x_{i-1} - \phi(x)), \qquad 1 \le i \le n, \tag{2}$$

where we have used that

$$\lim_{C\to\infty} \frac{C}{C+\phi(x)} = 1$$

because $\phi(x)$ is bounded. The term $\phi(x)$ is equivalent to the dilution outflow used in time-continuous models, which introduces competition between replicators also ensuring a constant population.

We note that for large values of C, the discrete system introduced above will have similar properties to system Eqs. (2). As mentioned, the main goal of our article is to investigate how dynamics change considering the range e.g., $k_1 \geq -1$ and $k_i > 0$ for $2 \leq i \leq n$. Due to the cyclic structure of hypercycles, setting a negative k_1 is the same that fixing any other single value of $k_{i\neq 1} \geq -1$ and all others to $k_{j\neq i} > 0$ (i.e., in this study we will focus on the change of sign of one parameter). A positive value of k_1 means that species x_1 receives catalytic aid from species x_n. For $k_1 = 0$ no interaction happens between x_1 and x_n, and the hypercycle becomes a catalytic chain (see [4]). For $k_1 < 0$, species x_n degrades species x_1 (i.e., by trans-cleaving ribozymes activity). Since we admit $k_1 \geq -1$, in order to have $C + \phi(x) > 0$ in S^{n-1} when $k_1 < 0$ we should take $C > -k_1/4$. This leads us to assume $C > 1/4$ in all cases.

III. RESULTS AND DISCUSSION

In the next Sections we will characterise the dynamics of Map (1). In Section A we will study the fixed points and their local stability. Section B discusses the behaviour of the system setting a negative k_1 value. In Section C we analyse the particular cases of two- three- and four-species systems, focusing on the dynamics and the bifurcations identified in the studied hypercycles. Section D provides analytical and numerical results of the rates of convergence to the point attractors. Finally, Section E provides a study on the invariant curves and the bifurcations for the case $n = 4$ when $k_1 = 0$.

A. Fixed poins and eigenvalues

We begin studying the fixed points of Map (1). In this work we assume $C > 1/4$, $k_1 \geq -1$ and $k_i > 0$ for $2 \leq i \leq n$. Let Δ^{n-1} be the hyperplane $\{x \in \mathbb{R}^n | \sum_{j=1}^n x_j = 1\}$. Note that $S^{n-1} \subset \Delta^{n-1}$. To understand the bifurcation that occurs when $k_1 = 0$ we consider F defined in $\Delta^{n-1} \setminus \{x \in \mathbb{R}^n | C + \phi(x) = 0\}$. For $k_1 \neq 0$ we introduce the quantity

$$M = \sum_{j=1}^{n} \frac{1}{k_j}.$$

Proposition 1. (a) *If $k_1 \neq 0$, $-1/(\sum_{j=2}^n \frac{1}{k_j})$, then F has a unique fixed point p^n in $\tilde{\Delta}^{n-1} = \{x \in \Delta^{n-1} | \, x_i \neq 0, \forall i\}$. We have*

$$p^n = (p_1, ..., p_n) \qquad with \quad p_i = \frac{1}{k_{i+1} M}, \quad 1 \leq i \leq n. \tag{3}$$

The point $p^n \in S^{n-1} \setminus \partial S^{n-1}$ if and only if $k_1 > 0$. Moreover, when $k_1 \to 0$, p^n converges to $(0, ..., 0, 1)$. If $k_1 = 0$ or $k_1 = -1/(\sum_{j=2}^n \frac{1}{k_j})$ then F has no fixed points in $\tilde{\Delta}^{n-1}$.

(b) *Let $x \in \Delta^{n-1} \setminus \tilde{\Delta}^{n-1}$. Then, x is a fixed point if and only if $k_i x_i x_{i-1} = 0$ for all i. If $k_1 > 0$ the previous conditions are also equivalent to $\phi(x) = 0$. The points $q^{n,m} = (q_1^m, \ldots, q_n^m)$ such that $q_i^m = \delta_{m,i}$, $0 \leq m \leq n$, are always fixed points (here δ is the Kronecker delta).*

Proof. (a). We assume $x_i \neq 0$ for all i. From the condition $F_i(x) = x_i$ we get

$$\frac{C + k_i x_{i-1}}{C + \phi(x)} = 1$$

and hence $k_i x_{i-1} = \phi(x)$ for all i. Then $k_2 x_1 = k_3 x_2 = ... = k_n x_{n-1} = k_1 x_n$. If $k_1 = 0$ there are no fixed points in $\tilde{\Delta}^{n-1}$. When $k_1 \neq 0$ we can write $x_i = (k_1/k_{i+1}) x_n$ and determine the value of x_n imposing the condition that the point is in Δ^{n-1}:

$$k_1 x_n \sum_{j=1}^{n-1} \frac{1}{k_{j+1}} + x_n = 1.$$

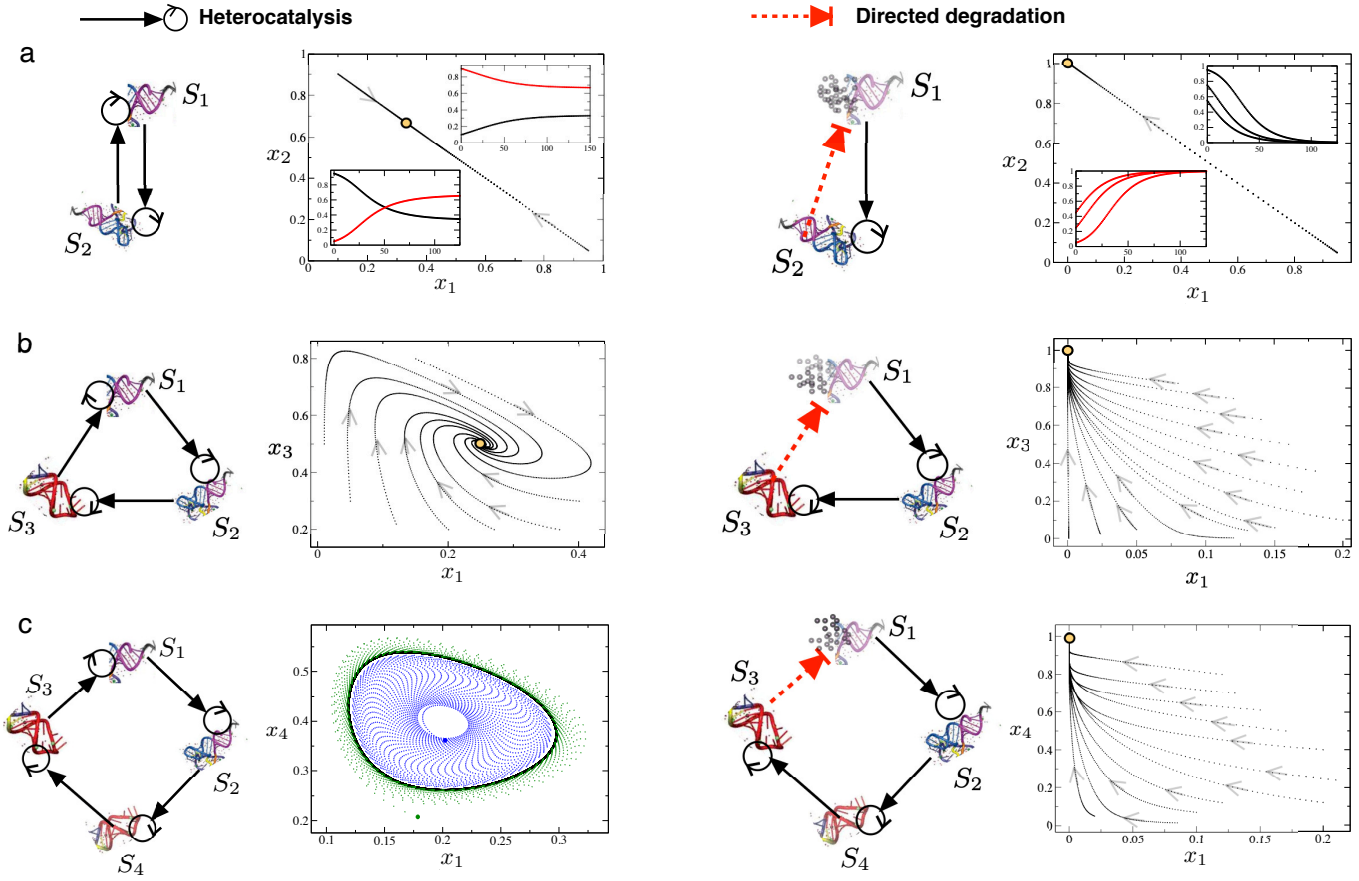

FIG. 1. Schematic diagram of the studied hypercycles formed by (ribozyme) species S_i (with $i = 2, ..., 4$) and their dynamical outcomes displayed in phase portraits considering cooperation (heterocatalysis represented with solid black arrows, setting $k_1 = 0.5$ and $k_{i\neq 1} = 1$), and emergence of directed degradation (trans-cleaving activity, indicated by dashed red arrows, using $k_1 = -0.5$ and $k_{i\neq 1} = 1$). (a) Two-member hypercycle: the insets display time series for x_1 (black) and x_2 (red) using the same initial conditions of the orbits of the phase portrait. The insets for directed degradation show time series also for x_1 (black) and x_2 (red) using different initial conditions that achieve the stable fixed point $q^{2,2} = (0, 1)$ (small orange dot). (b) Three-member hypercycle with a stable focus as coexistence attractor (fixed point p^3). The three-species system with directed degradation displays a stable fixed point at $q^{3,3} = (0, 0, 1)$. (c) Four-member hypercycle with oscillatory coexistence governed by an attracting invariant curve (shown in black). Two different initial conditions are shown: one spiralling towards (green iterations) the periodic attractor and another spiralling outwards (blue iterations) displayed in a two-dimensional projection. Directed degradation for this case has a single point attractor at $q^{4,4} = (0, 0, 0, 1)$. In all panels we have set $C = 10$.

If $k_1 = -1/\sum_{j=1}^{n-1} \frac{1}{k_{j+1}}$, there is not a fixed point in $\tilde{\Delta}^{n-1}$. Otherwise $k_1 x_n = 1/M$ and we get (3).

(b). Let $x \in \Delta^{n-1} \setminus \tilde{\Delta}^{n-1}$. There exists l such that $x_l = 0$ and $x_{l+1} \neq 0$. If x is a fixed point we have

$$x_{l+1} = \frac{C + k_{l+1}\, x_l}{C + \phi(x)} x_{l+1}$$

and hence $\phi(x) = k_{l+1}\, x_l = 0$. Therefore

$$x_i = \frac{C + k_i x_{i-1}}{C} x_i = x_i + \frac{1}{C}\, k_i\, x_i\, x_{i-1},$$

for all i and thus $k_i\, x_i\, x_{i-1} = 0$. Conversely, $k_i\, x_i\, x_{i-1} = 0$ for all i implies $\phi(x) = 0$ and one immediately gets that x is a fixed point. □

To obtain the eigenvalues of $DF(p^n)$ and study the stability of the fixed point p^n obtained in (a) of Proposition 1 it is convenient to use the following baricentric variables.

$$y_i = \frac{k_{i+1}\, x_i}{\sum_{j=1}^{n} k_{j+1}\, x_j}, \qquad 1 \leq i \leq n.$$

When $k_1 > 0$, this change of variables sends S^{n-1} to S^{n-1} bijectively and, more generally, for $k_1 \in \mathbb{R}$, sends the points of S^{n-1} except the ones on the hyperplane $\sum_{j=1}^n k_{j+1}\, x_j = 0$ to S^{n-1}. Whenever defined, i.e., when $\sum_{j=1}^n k_{j+1}\, x_j \neq 0$, the differential of the change has rank $n-1$ and, actually it is a (local) diffeomorphism from S^{n-1} to S^{n-1}. This means that we can compute the eigenvalues of DF at p^n in baricentric coordinates. In such coordinates F reads

$$F_i(y) = \frac{C + \frac{y_{i-1}}{\Psi(y)}}{C + \frac{1}{\Psi(y)} \sum_{j=1}^n y_{j-1}\, y_j}\, y_i, \qquad \text{where} \qquad \Psi(y) = \sum_{j=1}^n \frac{1}{k_{j+1}}\, y_j,$$

and the fixed point p^n located at $(1/n, ..., 1/n)$. It is not difficult to compute the partial derivatives and obtain

$$\frac{\partial F_i}{\partial y_i}(p^n) = 1 - \frac{2}{n(CM+1)}, \qquad \frac{\partial F_i}{\partial y_{i-1}}(p^n) = \frac{1}{CM+1} - \frac{2}{n(CM+1)}, \qquad \frac{\partial F_i}{\partial y_l}(p^n) = \frac{-2}{n(CM+1)}, \qquad l \neq i, i-1.$$

Then, the differential $DF(p^n)$ is a circulant matrix

$$\begin{pmatrix} c_0 & c_1 & \dots & c_{n-1} \\ c_{n-1} & c_0 & \dots & c_{n-2} \\ c_{n-2} & c_{n-1} & \dots & c_{n-3} \\ & & \dots & \\ c_1 & c_2 & \dots & c_0 \end{pmatrix} \tag{4}$$

with

$$c_0 = 1 - \frac{2}{n(CM+1)}, \;\; c_{n-1} = \frac{1}{CM+1} - \frac{2}{n(CM+1)}, \;\; \text{and} \;\; c_i = \frac{-2}{n(CM+1)} \;\; \text{for} \;\; 1 \leq i \leq n-2.$$

It is known [60] that the eigenvalues of a circulant matrix as (4) are

$$\lambda_m = \sum_{j=0}^{n-1} c_j\, e^{2\pi \mathrm{i} j m/n}, \qquad 0 \leq m \leq n-1,$$

where i denotes the imaginary unit $\sqrt{-1}$, with corresponding eigenvectors

$$(1, e^{-2\pi \mathrm{i} m/n}, ..., e^{-2\pi \mathrm{i}(n-1)m/n}).$$

In our case

$$\lambda_m = 1 + \frac{1}{CM+1}\, e^{2\pi \mathrm{i} m/n}, \qquad 0 \leq m \leq n-1.$$

The eigenvalue λ_0 corresponds to the eigenvector $(1, 1, ..., 1)$ which is transversal to S^{n-1}. The other eigenvalues correspond to eigenvectors tangent to S^{n-1}. Indeed, when $m \neq 0$, $\sum_{l=0}^{n-1} e^{-2\pi \mathrm{i} l m/n} = 0$.

To compute the eigenvalues of $DF(q^{n,n})$ we first look for the linearisation of F (in the original coordinates) at $q^{n,n} = (0, 0, ..., 1)$. To do so we translate it to the origin by means of the change of coordinates $x_n = \xi_n + 1$, $x_i = \xi_i$, $1 \leq i \leq n-1$. In these variables the map is expressed as:

$$\begin{aligned} \tilde{F}_1(\xi) &= \frac{C + k_1(\xi_n + 1)}{C + \tilde{\phi}(\xi)}\, \xi_1, \\ \tilde{F}_i(\xi) &= \frac{C + k_i \xi_{i-1}}{C + \tilde{\phi}(\xi)}\, \xi_i, \qquad 2 \leq i \leq n-1, \\ \tilde{F}_n(\xi) &= \frac{C + k_n \xi_{n-1}}{C + \tilde{\phi}(\xi)}\, (\xi_n + 1) - 1, \end{aligned}$$

where $\tilde{\phi}(\xi) = \sum_{j=1}^n k_j\, \xi_j\, \xi_{j-1} + k_1\, \xi_1 + k_n\, \xi_{n-1}$. From these expressions we readily obtain

$$DF(q^{n,n}) = \begin{pmatrix} 1 + \frac{k_1}{C} & 0 & \dots & 0 \\ 0 & 1 & \dots & 0 \\ & & \dots & \\ \frac{-k_1}{C} & 0 & \dots & 1 \end{pmatrix}.$$

The eigenvalues are $1 + k_1/C$ and 1. The eigenvalue $1 + k_1/C$ corresponds to the eigenvector $(1, 0, ..., 0, -1)$. The eigenvalue 1 corresponds to the (linearly independent) eigenvectors $(0, 1, -1, 0, ..., 0), (0, 1, 0, -1, ..., 0), ..., (0, 1, 0, ..., 0, -1)$ and $(0, ..., 0, 1)$. All these vectors are tangent to S^{n-1} except the last one. Proceeding in an analogous way we can check that the eigenvalues of $DF(q^{n,i})$ are $1 + k_{i+1}/C$ and 1.

B. When $k_1 \leq 0$ the basin of attraction of $q^{n,n}$ contains $S^{n-1} \setminus \partial S^{n-1}$

In this section we will prove that for $k_1 \leq 0$ the dynamics achieves the fixed point $q^{n,n}$. This involves that the species that performs directed degradation will outcompete all of the others. Let us go back to Map (1). As mentioned, by the cyclic structure of the map we only deal with the case $k_1 \leq 0$. But, by the symmetry, in the same way we have that if $k_j \leq 0$ and $k_{i\neq j} > 0$ the dynamics achieves $q^{j-1,j-1}$. We now assume that $-1 \leq k_1 \leq 0$, and $k_i > 0$ for $2 \leq i \leq n$. These conditions ensure that for $x \in S^{n-1}$ both $C + k_i x_{i-1}$ and $C + \phi(x)$ are positive.

Proposition 2. *Assume $C > 1/4$, $-1 \leq k_1 \leq 0$, and $k_i > 0$ with $2 \leq i \leq n$. If $x^0 \in S^{n-1} \setminus \partial S^{n-1}$ then $\{F^m(x^0)\}$ converges to $q^{n,n} = (0, 0, ..., 1)$.*

Proof. We write $x^m = (x_1^m, ..., x_n^m) = F^m(x^0)$. Since $x^0 \notin \partial S^{n-1}$, $0 < x_i^0 < 1$ for all i. Moreover, by the form of F, $0 < x_i^m < 1$ for all m and i. First, we check that $\{x_1^m\}$ is strictly decreasing and converges to 0. Indeed, since $k_1 \leq 0$ and $x_1^m < 1$, $k_1 x_n^m x_1^m \geq k_1 x_n^m$ and since $k_i > 0$ for $2 \leq i \leq n$, $\phi(x^m) > k_1 x_n^m$. Then

$$0 < \frac{C + k_1 x_n^m}{C + \phi(x^m)} < 1 \qquad \text{and} \qquad x_1^{m+1} = \frac{C + k_1 x_n^m}{C + \phi(x^m)}\, x_1^m < x_1^m, \quad m \geq 1.$$

By compactness of S^{n-1} there is a subsequence $\{x^{m_k}\}$ of $\{x^m\}$ which converges to some $\tilde{x} = (\tilde{x}_1, ..., \tilde{x}_n) \in S^{n-1}$. Note that, by monotonicity, $\{x_1^m\}$ converges to $\tilde{x}_1$. We assume that $\tilde{x}_1 > 0$ to get a contradiction. Taking limit in

$$x_1^{m_k+1} = \frac{C + k_1 x_n^{m_k}}{C + \phi(x^{m_k})} x_1^{m_k}$$

we get

$$\frac{C + k_1 \tilde{x}_n}{C + \phi(\tilde{x})} = 1$$

which implies $k_1 \tilde{x}_n = \phi(\tilde{x})$, or equivalently $k_1 \tilde{x}_n (1 - \tilde{x}_1) = k_2 \tilde{x}_2 \tilde{x}_1 + k_3 \tilde{x}_3 \tilde{x}_2 + \cdots + k_n \tilde{x}_n \tilde{x}_{n-1}$. The left hand side is less or equal than zero while the right hand one is bigger or equal than zero. Therefore $k_i \tilde{x}_i \tilde{x}_{i-1} = 0$, $2 \leq i \leq n$, and, in particular, $\tilde{x}_2 \tilde{x}_1 = 0$ which gives $\tilde{x}_2 = 0$.

From

$$\frac{x_1^{m+1}}{x_2^{m+1}} = \frac{C + k_1 x_n^m}{C + k_2 x_1^m}\, \frac{x_1^m}{x_2^m}$$

and

$$0 < \frac{C + k_1 x_n^m}{C + k_2 x_1^m} < 1$$

we have that $\left\{\frac{x_1^m}{x_2^m}\right\}$ is strictly decreasing, in particular is bounded from above. Then

$$x_1^{m_k} = \frac{x_1^{m_k}}{x_2^{m_k}}\, x_2^{m_k}$$

converges to 0 which provides the desired contradiction.

Now, we claim that, for $1 \leq i \leq n-1$, $\left\{\frac{x_i^m}{x_{i+1}^m}\right\}$ is strictly monotone for $m \geq M$ for some M (depending on i) and $x_i \to 0$. Indeed, by the previous arguments the statement is true for $i = 1$. We assume it is true for $1 \leq i \leq n-2$. Let

$$\gamma_i = \lim_{m \to \infty} \frac{k_{i+1} x_i^m}{k_{i+2} x_{i+1}^m}, \qquad 1 \leq i \leq n-2.$$

Note that $0 \leq \gamma_i \leq \infty$. If $\gamma_i > 1$, or $\gamma_i = 1$ and $\left\{\frac{x_i^m}{x_{i+1}^m}\right\}$ is decreasing, then

$$\frac{k_{i+1}\, x_i^m}{k_{i+2}\, x_{i+1}^m} > 1,$$

for $m \geq \tilde{M}$ for some $\tilde{M}$ and then $\left\{\frac{x_{i+1}^m}{x_{i+2}^m}\right\}$ is strictly increasing for $m \geq \tilde{M}$.

If $\gamma_i < 1$, or $\gamma_i = 1$ and $\left\{\frac{x_i^m}{x_{i+1}^m}\right\}$ is increasing, then

$$\frac{k_{i+1}\, x_i^m}{k_{i+2}\, x_{i+1}^m} < 1,$$

for $m \geq \hat{M}$ for some $\hat{M}$ and then $\left\{\frac{x_{i+1}^m}{x_{i+2}^m}\right\}$ is strictly decreasing for $m \geq \hat{M}$.

Now, to prove that $\{x_{i+1}^m\}$ converges to zero we distinguish two cases: $\gamma_i > 0$ and $\gamma_i = 0$.

When $\gamma_i > 0$ there exists m_i^0 such that

$$\frac{k_{i+1}x_i^m}{k_{i+2}x_{i+1}^m} > \frac{\gamma_i}{2}, \qquad m \geq m_i^0,$$

and then, from

$$x_{i+1}^m < \frac{k_{i+1}}{k_{i+2}}\,\frac{2}{\gamma_i}\, x_i^m,$$

we get $x_{i+1}^m \to 0$.

When $\gamma_i = 0$, there exists $\tilde{m}_i^0$ such that

$$\frac{k_{i+1}x_i^m}{k_{i+2}x_{i+1}^m} < \frac{1}{2} \qquad \text{for} \qquad m \geq \tilde{m}_i^0.$$

Obviously, for $m \geq \tilde{m}_i^0$,

$$\frac{C + k_{i+1}x_i^m}{C + k_{i+2}x_{i+1}^m} < \frac{C + (1/2)k_{i+2}x_{i+1}^m}{C + k_{i+2}x_{i+1}^m} < 1.$$

If we assume that $\{x_{i+1}^m\}$ does not converge to 0, then there exists $\varepsilon > 0$ and infinitely many indices m such that $k_{i+2}x_{i+1}^m > \varepsilon$ and therefore infinitely many factors

$$\frac{C + k_{i+1}x_i^m}{C + k_{i+2}x_{i+1}^m} < \frac{C + (1/2)\varepsilon}{C + \varepsilon}.$$

This means that, given q,

$$\frac{x_{i+1}^m}{x_{i+2}^m} < \left(\frac{C + (1/2)\varepsilon}{C + \varepsilon}\right)^{q_m}\, \frac{x_{i+1}^q}{x_{i+2}^q}, \qquad m > q,$$

with $q_m \to \infty$ as $m \to \infty$. Clearly, $\left\{\frac{x_{i+1}^m}{x_{i+2}^m}\right\} \to 0$ and $x_{i+1}^m < \frac{x_{i+1}^m}{x_{i+2}^m}$ gives that $\{x_{i+1}^m\}$ converges to 0.

Finally, since $x^m \in S^{n-1}, x_n^m \to 1$. □

C. Case studies: Hypercycles with n=2, n=3, and n=4 members

1. *Case n=2*

In this case the model is essentially one dimensional. When $k_i > 0$ it has a unique inner fixed point

$$p^2 = \left(\frac{k_1}{k_1 + k_2}, \frac{k_2}{k_1 + k_2}\right),$$

and the fixed points $q^{2,1} = (1, 0)$ and $q^{2,2} = (0, 1)$. The eigenvalue at p is

$$1 + \frac{1}{CM + 1}e^{2\pi \mathrm{i}/2} = \frac{CM}{CM + 1} = \frac{C(k_1 + k_2)}{C(k_1 + k_2) + k_1k_2} < 1.$$

The eigenvalues at $q^{2,1}$ and $q^{2,2}$ are $1 + k_2/C$ and $1 + k_1/C$, respectively. Actually, p^2 attracts all points of $S^1 \setminus \partial S^1$. When $k_1 \to 0$ with k_2 fixed, the fixed point p^2 tends to $q^{2,2}$ and they undergo a transcritical bifurcation. When $k_1 \leq 0$ all points of $S^1 \setminus \partial S^1$ tend to $q^{2,2}$. The bifurcation diagram obtained by iteration of Map (1) and tuning $-1 \leq k_1 \leq 1$ is displayed in Fig. 2(a). Here, for $0 < k_1 \leq 1$ the coexistence equilibrium is given by the fixed point p^2. At $k_1 = 0$ the points p^2 and $q^{2,2}$ collide in a transcritical bifurcation. Then, for negative values of k_1 the point $q^{2,2}$ is stable.

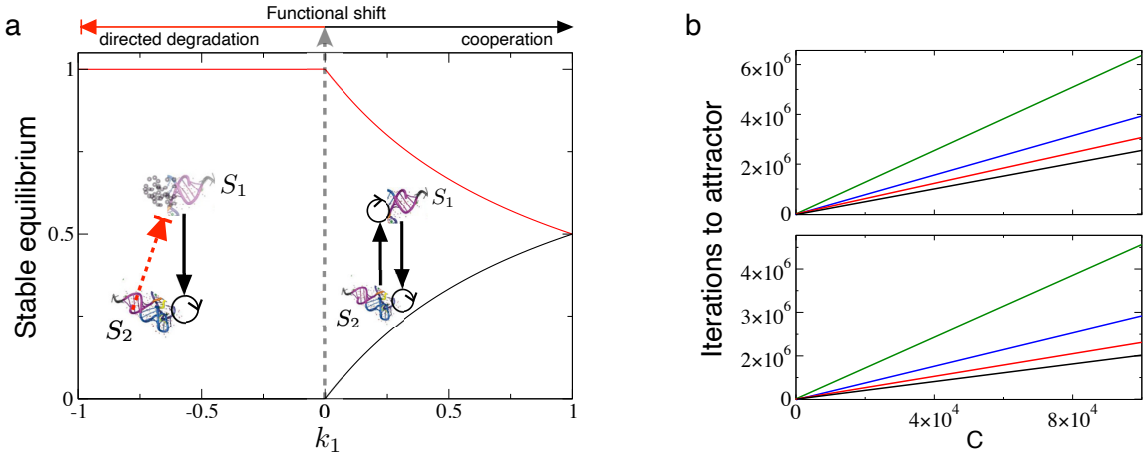

FIG. 2. (a) Bifurcation diagram obtained by iteration of Map (1) when $n = 2$ using k_1 as a control parameter with $k_2 = 1$ and $C = 10$. Black and red lines denote the equilibrium population of species x_1 and x_2 respectively. For $0 < k_1 \leq 1$ the dynamics is attracted by the fixed point p^2, while for $-1 \leq k_1 < 0$ the stable fixed point is $q^{2,2}$, involving the persistence of the second replicator and the extinction of S_1. At $k_1 = 0$ the fixed points p^2 and $q^{2,2}$ collide in a transcritical bifurcation. (b) Linear dependence of parameter C on the number of iterations needed to achieve the attractors fixing $k_2 = 1$ and: (upper panel, for attractor p^2) $k_1 = 1$ (black), $k_1 = 0.75$ (red), $k_1 = 0.5$ (blue), $k_1 = 0.25$ (green); (lower panel, for attractor $q^{2,2}$) we have used the same values of k_1 than in the upper panel but with negative sign. We consider $\delta = 10^{-6}$. In all panels we have used $x_1(0) = 0.75, x_2(0) = 0.25$ as initial conditions.

2. *Case n=3*

When $k_i > 0$ the inner fixed point is given by

$$p^3 = \left(\frac{1}{k_2 M}, \frac{1}{k_3 M}, \frac{1}{k_1 M}\right),$$

and the corresponding eigenvalues are

$$\lambda_{1,2} = 1 + \frac{1}{CM+1} e^{i\theta_{1,2}}, \qquad \theta_1 = \frac{2\pi}{3}, \quad \theta_2 = \frac{4\pi}{3}.$$

We have

$$|\lambda_{1,2}|^2 = 1 + \frac{2}{CM+1}\cos\theta_{1,2} + \left(\frac{1}{CM+1}\right)^2 = 1 - \frac{1}{CM+1}\left(1 - \frac{1}{CM+1}\right) < 1.$$

The other fixed points, according to Proposition 1, satisfy $\phi(x) = 0$. The only possibilities are $q^{3,1} = (1,0,0)$, $q^{3,2} = (0,1,0)$ and $q^{3,3} = (0,0,1)$. They have an eigenvalue of modulus greater than 1. The point p^3 is an attractor. In Ref. [55] it is proved, by using a strict Lyapunov function, that $S^2 \setminus \partial S^2$ is the basin of attraction of p^3. When $k_1 \to 0$ with k_2 and k_3 fixed, p^3 tends to $q^{3,3}$ and they undergo a (degenerate) transcritical bifurcation. At the bifurcation, the two eigenvalues are 1. A special feature is that at the bifurcation there is a segment of fixed points $\{x_2 = 0, x_1 + x_3 = 1\}$ with $q^{3,3}$ in an extreme of it. After the bifurcation, i.e., when $k_1 < 0$, p^3 is outside S^2, it is unstable. Moreover, when $k_1 \leq 0$, $q^{3,3}$ attracts all points of $S^2 \setminus \partial S^2$. The dynamics for $n = 3$ is displayed in Fig. 3(a) by means of a bifurcation diagram built iterating Map (1). Here, similarly to the case $n = 2$, the hypercycle persists for $0 < k_1 \leq 1$ because the point p^3 is stable. At $k_1 = 0$, there is a degenerate transcritical bifurcation between the points p^3 and $q^{3,3}$, and for negative values of k_1 the third member outcompetes all other species i.e., the fixed point $q^{3,3}$ attracts all points of $S^2 \setminus \partial S^2$.

3. *Case n=4*

For $k_i > 0$ the dynamics is governed by an invariant curve [55, 56] that allows the coexistence of all of the species by means of an oscillatory regime (see Figs. 1, 4(a), and 6). When $k_i > 0$, the inner fixed point is given by

$$p^4 = \left(\frac{1}{k_2 M}, \frac{1}{k_3 M}, \frac{1}{k_4 M}, \frac{1}{k_1 M}\right),$$

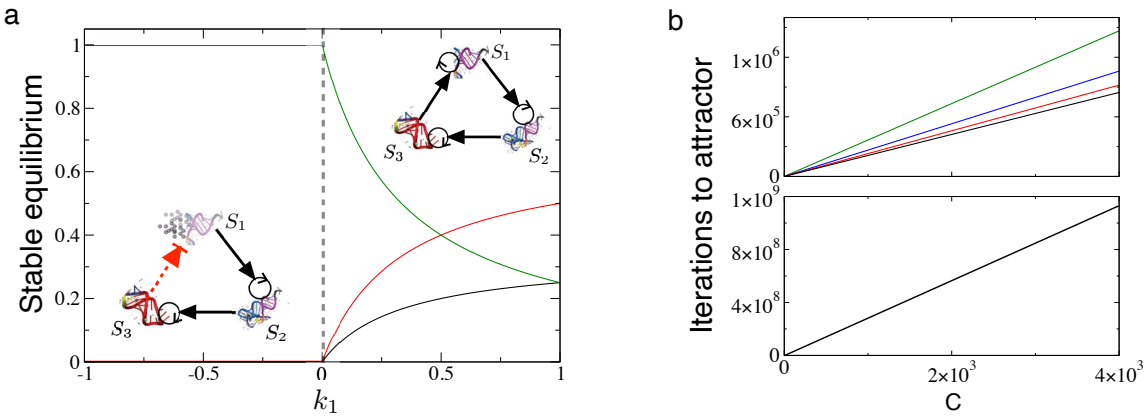

FIG. 3. (a) Bifurcation diagram obtained by iteration of Map (1) when $n = 3$ using k_1 as a control parameter with $k_2 = 1, k_3 = 0.5$, and $C = 10$. Here we show equilibria for variables x_1 (black), x_2 (red), and x_3 (green). For positive k_1 the dynamics achieve the fixed point p^3. At $k_1 = 0$ there is a degenerate transcritical bifurcation between the fixed points p^3 and $q^{3,3}$. For negative k_1 the fixed point $q^{3,3}$ is an attractor. (b) Linear dependence of parameter C on the number of iterations needed to achieve the attractor $q^{3,3}$ fixing $k_2 = 1$ and: (upper panel, for attractor p^3) $k_1 = 1$ (black), $k_1 = 0.75$ (red), $k_1 = 0.5$ (blue), $k_1 = 0.25$ (green); (lower panel, for attractor $q^{3,3}$) here we have used $k_1 = -1$. Due to the extremely long transients obtained for $k_1 < 0$ we here consider $\delta = 10^{-5}$ and a shorter range for C. Here the four values of $k_1 < 0$ give place to very similar transient times, which are displayed overlapped and also have a linear dependence on C. In all panels we have used $x_1(0) = 0.5, x_2(0) = 0.35$, and $x_3(0) = 0.15$ as initial conditions.

and its eigenvalues are

$$\lambda_j = 1 + \frac{1}{CM+1} e^{\mathrm{i}\theta_j} \qquad \text{with} \qquad \theta_j = e^{\mathrm{i}2\pi j/4}, \quad 1 \le j \le 3.$$

We have

$$|\lambda_1|^2 = |\lambda_3|^2 = 1 + \left(\frac{1}{CM+1}\right)^2 > 1 \qquad \text{and} \qquad |\lambda_2|^2 = \left(1 - \frac{1}{CM+1}\right)^2 < 1.$$

Moreover, on ∂S^3 we have the fixed points $q^{4,i}$, with $q_i^{4,i} = \delta_{ij}$ (δ being the Kronecker delta) and the segments of fixed points $\{(\alpha, 0, 1-\alpha, 0) | \, \alpha \in [0,1]\}, \{(0, \alpha, 0, 1-\alpha) | \, \alpha \in [0,1]\}$. When $k_1 = 0$ we also have the segment of fixed points $\{(\alpha, 0, 0, 1-\alpha) | \, \alpha \in [0,1]\}$. When $k_1 \to 0$, p tends to $q^{4,4}$ and at the bifurcation value $k_1 = 0$ all eigenvalues are equal to 1. At the bifurcation and after it, i.e. when $k_1 \le 0$, $q^{4,4}$ attracts all points of $S^3 \setminus \partial S^3$.

Figure 4 displays how local maxima and minima obtained from time series for the dynamics on the invariant curve change at decreasing k_1 from 1 to 0. Notice that the invariant curve shrinks (see also Fig. 6(a)), finally collapsing at $k_1 = 0$ (the stability of the invariant curve as well as the bifurcations occurring at crossing $k_1 = 0$ are discussed in Section III E below).

D. Rates of convergence to the point attractors

In this section we study the rates of convergence of the point attractors of the system. For that, given an initial condition $x^0 \in S^{n-1} \setminus \partial S^{n-1}$, we compute the number of iterations m to arrive to a ball of radius δ centered at the attractor. We have several cases depending on m and on whether the attractor is the inner point or a vertex. Also, the computations are different if the fixed point is hyperbolic or not. For $n = 2$ and $n = 3$, if $k_1 > 0$, the attractors are p^2 and p^3, respectively, which are hyperbolic. If $k_1 \le 0$, the attractors are $q^{2,2}$ and $q^{3,3}$. The point $q^{2,2}$ is hyperbolic if $k_1 < 0$ while both $q^{2,2}$ and $q^{3,3}$ have eigenvalues equal to one in the other cases. When $n = 4$, if $k_1 > 0$, there is not an attracting fixed point. If $k_1 \le 0$, the attractor is $q^{4,4}$, which has eigenvalues equal to 1. Here attractor is understood as a fixed point, which attracts all points of the interior of the simplex. Notice that, in some cases, they have eigenvalues equal to 1. Together with the analytical derivations developed along this section, we also provide numerical results computing the number of iterations to achieve the attractors, showing their linear dependence with the discretisation parameter C (and with replication constants, see below). Specifically, Fig. 2(b) displays this linear relation between

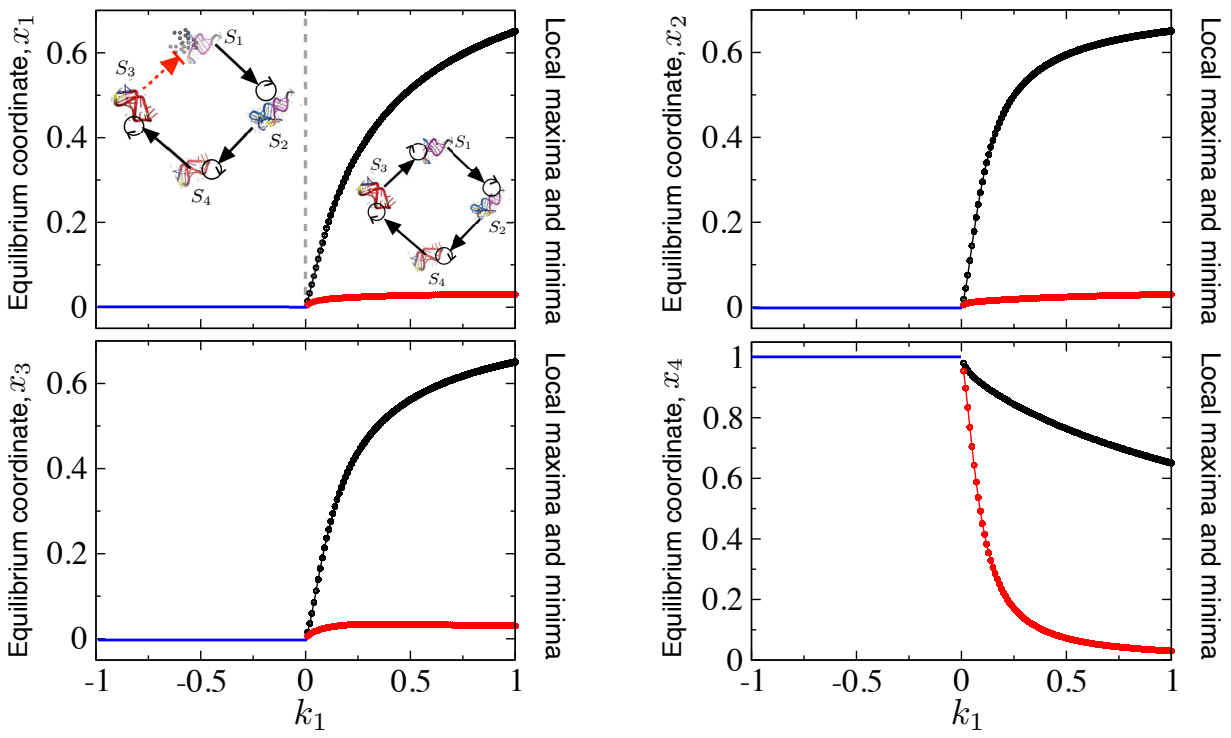

FIG. 4. Bifurcation diagram for the four-member hypercycle obtained by iteration of Map (1) using $-1 \leq k_1 \leq 1$ as control parameter, setting $k_{2,3,4} = 1$ and using the initial condition $x_0(0) = x_1(0) = x_2(0) = 0.025$ and $x_4(0) = 0.925$. The black and red dots display, respectively, the local maxima and minima of each variable obtained from time series once the dynamics has settled on the invariant curve for $k_1 > 0$ (right y-axis). For $1 \leq k_1 < 0$, the equilibrium of each coordinate is also displayed (left y-axis). Here the only species that persists is x_4. In all panels we set $C = 10$.

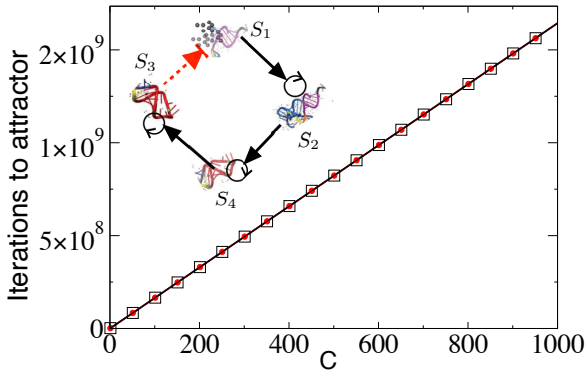

FIG. 5. Number of iterations to reach the attractor $q^{4,4}$ for $n = 4$ and their relation with C, setting $1 \leq C \leq 10^3$ and $k_2 = 1$, $k_3 = 0.5$, $k_4 = 1$, with; $k_1 = -1$ (black line), $k_1 = -0.8$ (red) dots, and $k_1 = -0.6$ (black squares). Here we have used $\delta = 10^{-6}$ and the initial conditions $x_0(0) = x_1(0) = x_2(0) = 0.025$ and $x_4(0) = 0.925$. See Section III D for details.

C and the iterations to the coexistence attractor p^2 (upper panel) and to the out-competition attractor $q^{2,2}$ (lower panel). Also, we have found the linear relation between C and the iterations to the coexistence attractor p^3 (upper panel in Fig. 3(b)) and the out-competition one $q^{3,3}$ (lower panel in Fig. 3(b)). Finally, Fig. 5 also displays the linear relation between constant C and the out-competition attractor $q^{4,4}$. Specifically, we have obtained that for the points p^2, p^3 the times are proportional to $C(\sum_{i=1}^{n} \frac{1}{k_i})$, $n = 2, 3$, and for the points $q^{n,n}$, $n = 2, 3, 4$, the times are proportional to C/k_n.

Next, we describe in detail the computation of the number of iterations in the more involved cases i.e., for p^3 when

$n = 3$ and $q^{4,4}$ when $n = 4$. The other cases are studied using the same ideas in a much simpler way. For the latter we will just make some comments on the variations on the arguments and give the results.

1. *Convergence to p^3*

When $n = 3$ the system is essentially two dimensional. We use the variables x_1, x_2 to describe S^2. The eigenvalues at p^3 have already been computed and are

$$\lambda_1 = 1 - \frac{1}{2(CM+1)} + \mathrm{i}\frac{\sqrt{3}}{2(CM+1)}, \qquad \lambda_2 = \bar{\lambda}_1,$$

with

$$|\lambda_1| = |\lambda_2| = 1 - \frac{1}{CM+1} + \frac{1}{(CM+1)^2} < 1.$$

Since p^3 is a hyperbolic attractor (without resonances) we can apply Poincaré's theorem [61] and get that the system is locally conjugated to its linear part L by an analytical conjugation h defined in a neighbourhood of 0 sending 0 to p_3 and satisfying $Dh(0) = \mathrm{Id}$. Specifically, we have

$$F \circ h = h \circ L \qquad \text{in a neighbourhood of } 0. \tag{5}$$

From basic algebra we know that there exists a non-singular matrix B such that $B^{-1} L B = \tilde{L}$ with

$$\tilde{L} = |\lambda_1| \begin{pmatrix} \cos\varphi_1 & -\sin\varphi_1 \\ \sin\varphi_1 & \cos\varphi_1 \end{pmatrix}, \qquad \varphi_1 = \arg\lambda_1.$$

Clearly,

$$\tilde{L}^m = |\lambda_1|^m \begin{pmatrix} \cos(m\varphi_1) & -\sin(m\varphi_1) \\ \sin(m\varphi_1) & \cos(m\varphi_1) \end{pmatrix}.$$

We take $\tilde{h} = h \circ B$ and we have

$$F \circ \tilde{h} = F \circ h \circ B = h \circ L \circ B = h \circ B \circ \tilde{L} = \tilde{h} \circ \tilde{L}. \tag{6}$$

We assume that $\tilde{h}$ is defined in a ball of radius r, $B_r(0)$. Using (6) we can extend the domain of $\tilde{h}$ to a neighbourhood $\mathcal{U}$ of 0 such that $\tilde{h}(\mathcal{U})$ is contained in the image by F of its domain of invertibility. Indeed, we start with $\tilde{h}$ defined on $B_r(0)$ and we inductively use $\tilde{h} = F^{-1} \circ \tilde{h} \circ \tilde{L}$ to extend, at step j, the domain of $\tilde{h}$ from $B_{|\lambda_1|^{-j+1}r}(0)$ to $B_{|\lambda_1|^{-j}r}(0)$. This can be done while F^{-1} exists. Then, eventually we have to stop at some step j_0. Notice that if the parameter C is big enough, F is globally invertible in the simplex and in such case the domain of $\tilde{h}$ can be extended to $\mathbb{R}^2$.

We denote $\mathcal{U} = \tilde{h}\left(B_{|\lambda|^{-j_0}r}(0)\right)$. Let $x^0 \in S^2 \setminus \partial S^2$. Since p^3 is a global attractor (Theorem 3 of [55]) there exists $m_0 \geq 1$ such that $F^{m_0}(x^0) \in \mathcal{U}$. We can write

$$F^m(x^0) = F^{m-m_0}(F^{m_0}(x^0)) = F^{m-m_0}(\tilde{h}(y^0)), \qquad m \geq m_0$$

for some $y^0 \in B_{|\lambda|^{-j_0}r}(0)$. Then

$$\|F^m(x^0) - p^3\| = \|F^{m-m_0}(\tilde{h}(y^0)) - \tilde{h}(0)\| = \|\tilde{h} \circ \tilde{L}^{m-m_0}(y^0) - \tilde{h}(0)\|.$$

Since we look for m such that $\tilde{L}^{m-m_0}\, y^0$ is very close to 0 and we have $D\tilde{h}(0) = B$,

$$\|B^{-1}\|^{-1}\, \|\tilde{L}^{m-m_0}\, y^0\| \lesssim \|\tilde{h} \circ \tilde{L}^{m-m_0}(y^0) - \tilde{h}(0)\| \lesssim \|B\|\, \|\tilde{L}^{m-m_0}(y^0)\|.$$

Moreover, $\|\tilde{L}^{m-m_0}\, y^0\| = \delta$ is equivalent to

$$m = \frac{\log\delta - \log\|y^0\|}{\log|\lambda_1|} + m_0.$$

If C is big,

$$\log|\lambda_1| = \frac{-1}{CM} + \frac{3}{2}\frac{1}{(CM)^2} - \frac{1}{3}\frac{1}{(CM)^3} + \mathcal{O}\left(\frac{1}{(CM)^4}\right),$$

and then m is of the order $CM(\log\delta^{-1} - \log\|\tilde{h}^{-1}(F^{m_0}(x^0))\|^{-1}) + m_0$.

Here, and in the following cases, $\log\tilde{h}^{-1}(F^{m_0}(x^0))$ should be interpreted as a constant depending on the initial condition.

2. Convergence to p^2 (when $k_1 > 0$)

In this case p^2 is a hyperbolic fixed point ($k_1 > 0$) and the corresponding eigenvalue is $\lambda = (CM)/(1+CM)$. Using the same strategy as before, we obtain

$$m \approx \frac{\log \delta - \log \tilde{h}^{-1}(F^{m_0}(x^0))}{\log \lambda} + m_0 =$$
$$= CM\Big[\log \delta^{-1} - \log(\tilde{h}^{-1}(F^{m_0}(x^0)))^{-1}\Big]\left(1 + \mathcal{O}\left(\frac{1}{CM}\right)\right) + m_0.$$

3. Convergence to $q^{2,2}$ (when $k_1 < 0$)

The eigenvalue corresponding to $q^{2,2}$ is $1 + k_1/C < 1$. Similarly as before we now have

$$m \approx \frac{C}{(-k_1)}\Big[\log \delta^{-1} - \log(\tilde{h}^{-1}(F^{m_0}(x^0)))^{-1}\Big]\left(1 + \mathcal{O}\left(\frac{k_1}{C}\right)\right) + m_0.$$

4. Convergence to $q^{4,4}$ (when $k_1 \leq 0$)

The point $q^{4,4}$ is not hyperbolic and this fact forces to introduce several technicalities. We start with a lemma which provides control on the convergence of some sequences.

Lemma 3. *Let $\gamma > 0$, $m_0 \geq 0$ and $\{z^m\}$ be a sequence of positive numbers. If $z^{m+1} \geq \frac{z^m}{1+\gamma z^m}$ for $m \geq m_0$ then*

$$z^m \geq \frac{z^{m_0}}{1 + (m - m_0)\gamma z^{m_0}}, \qquad m \geq m_0.$$

If $z^{m+1} \leq \frac{z^m}{1+\gamma z^m}$ for $m \geq m_0$ then

$$z^m \leq \frac{z^{m_0}}{1 + (m - m_0)\gamma z^{m_0}}, \qquad m \geq m_0.$$

The same statement is true with strict inequalities with the conclusions for $m > m_0$.

Proof. Let $\{\xi^m\}$ be the auxiliary sequence defined by $\xi^{m_0} = z^{m_0}$ and

$$\xi^{m+1} = \frac{\xi^m}{1 + \gamma \xi^m}, \qquad m \geq m_0.$$

We easily check by induction that $\xi^m = \frac{\xi^{m_0}}{1+(m-m_0)\gamma \xi^{m_0}}$. We claim that $z^m \geq \xi^m$ for all $m \geq m_0$. Indeed, when $m = m_0$ this is obviously true. Assuming it is true for $m \geq m_0$, and using that $\varphi(t) = \frac{t}{1+\gamma t}$ is strictly increasing in $(0, \infty)$ we have

$$z^{m+1} \geq \frac{z^m}{1 + \gamma z^m} \geq \frac{\xi^m}{1 + \gamma \xi^m} = \xi^{m+1}.$$

Then the result is obtained. The second part follows in the same way. □

Let $(x_1^0, x_2^0, x_3^0, x_4^0) \in S^3 \setminus \partial S^3$. We already know from the proof of Proposition 2 that the sequences $\{x_1^m/x_2^m\}$, $\{x_2^m/x_3^m\}$ and $\{x_3^m/x_4^m\}$ are strictly monotone from some index on, that $\{x_1^m\}$, $\{x_2^m\}$, $\{x_3^m\}$ converge to 0 and $\{x_4^m\}$ converges to 1.

In the next claims we will use a small constant $\varepsilon > 0$ and an integer m_0 sufficiently big. They will be the ones needed for certain conditions on sequences to be met, and may be different at different places. We will require a finite (small) number of such conditions. Given $\varepsilon \in (0, 1)$ there exists m_0 such that $x_1^m < \varepsilon$, $x_2^m < \varepsilon$, $x_3^m < \varepsilon$ and $x_4^m > 1 - \varepsilon$ for $m \geq m_0$. Since $\{x_1^m/x_2^m\}_{m \geq 0}$ is strictly decreasing, $x_1^m/x_2^m < \beta_1$ for some $\beta_1 > 0$.

Moreover, since $x_3^m/x_4^m \to 0$, $\{x_3^m/x_4^m\}$ is strictly decreasing for $m \geq m_0$, then $\frac{C+k_3 x_2^m}{C+k_4 x_3^m} < 1$ and hence $k_3 x_2^m < k_4 x_3^m$ for $m \geq m_0$.

Claim 4. $\{x_1^m/x_3^m\}_{m\geq 0}$ *converges to 0.*

Proof. First we consider the case $k_1 = 0$. We have that

$$\frac{x_1^{m+1}}{x_3^{m+1}} = \frac{C}{C + k_3 x_2^m}\frac{x_1^m}{x_3^m}$$

and hence $\{\frac{x_1^m}{x_3^m}\}_{m\geq 0}$ is strictly decreasing. We know that $x_1^m \leq \beta_1 x_2^m$.

To get a contradiction we assume that $\lim_{m\to\infty} x_1^m/x_3^m = \beta_2 > 0$. Then $x_1^m > \beta_2 x_3^m$ for $m \geq 0$ and $\phi(x^m) = k_2 x_2^m x_1^m + k_3 x_3^m x_2^m + k_4 x_4^m x_3^m < (k_2 + k_3/\beta_2 + k_4/\beta_2)x_1^m$. Then $x_1^{m+1} = \frac{C}{C+\phi(x^m)}x_1^m > \frac{1}{1+\gamma_1 x_1^m}x_1^m$, where $\gamma_1 = (k_2 + k_3/\beta_2 + k_4/\beta_2)/C$ for all $m \geq 0$. By Lemma 3, $x_1^m > x_1^0/(1 + m\gamma_1 x_1^0)^{-1}$. Then

$$\frac{x_1^m}{x_3^m} = \left(\prod_{j=0}^{m-1}\frac{C}{C + k_3 x_2^j}\right)\frac{x_1^0}{x_3^0} = \left(\exp\sum_{j=0}^{m-1}\log\frac{C}{C + k_3 x_2^j}\right)\frac{x_1^0}{x_3^0}. \tag{7}$$

Assume ε is small enough so that $(k_3/(\beta_1 C))\varepsilon < 1$. Using that $\log\frac{1}{1+t} < -(\log 2)t$ for $t \in (0,1)$ we have $\log\frac{C}{C+k_3 x_2^j} < \log\frac{C}{C+(k_3/\beta_1)x_1^j} < -(\log 2)(k_3/(\beta_1 C))x_1^j < -(\log 2)(k_3/(\beta_1 C))\frac{x_1^0}{1+j\gamma_1 x_1^0}$ for $m \geq 0$ and therefore the sum in (7) diverges to $-\infty$ when $m \to \infty$ and hence $\frac{x_1^m}{x_3^m} \to 0$ which is a contradiction.

When $k_1 < 0$, we use that given $\varepsilon > 0$ there exists m_0 such that if $m \geq m_0$ then $x_4^m > 1 - \varepsilon$. Then

$$\frac{x_1^{m+1}}{x_3^{m+1}} \leq \frac{C + k_1(1-\varepsilon)}{C}\frac{x_1^m}{x_3^m}, \qquad m \geq m_0.$$

Since $\frac{C+k_1(1-\varepsilon)}{C} < 1$, we also have $\frac{x_1^m}{x_3^m} \to 0$.

□

Claim 5. $\{x_2^m/x_3^m\}_{m\geq 0}$ *converges to 0.*

Proof. We assume that $\lim x_2^m/x_3^m = \beta_3 > 0$. By the condition $k_3 x_2^m < k_4 x_3^m$ for $m \geq m_0$ we have $\beta_3 \leq k_4/k_3$.

Then $x_2^m > (\beta_3 - \varepsilon)x_3^m$ for $m > m_0$. Moreover, since $x_1^m/x_3^m < \varepsilon$ for $m \geq m_0$ we also have that $x_1^m < (\varepsilon/(\beta_3 - \varepsilon))x_2^m$. Then $\phi(x^m) \leq k_2 x_2^m x_1^m + k_3 x_3^m x_2^m + k_4 x_4^m x_3^m < (k_2 + k_3 + k_4/(\beta_3 - \varepsilon))x_2^m$. Then $x_2^{m+1} = \frac{C+k_2 x_1^m}{C+\phi(x^m)}x_2^m > \frac{1}{1+\gamma_3 x_2^m}x_2^m$, where $\gamma_3 = (k_2 + k_3 + k_4/(\beta_3 - \varepsilon))/C$ for all $m \geq m_0$.

By Lemma 3, $x_2^m \geq \frac{x_2^{m_0}}{1+(m-m_0)\gamma_3 x_2^{m_0}}$ for $m \geq m_0$. Moreover, using again that $k_3 x_2^m < k_4 x_3^m$,

$$x_3^m \geq \frac{(k_3/k_4)x_2^{m_0}}{1 + (m - m_0)\gamma_3 x_2^{m_0}}. \tag{8}$$

On the other hand, using that if $A > 0$ and $-1 + 2A < B < 1 + 2A$

$$\frac{1+A}{1+B} < \frac{1}{1+B-2A}, \tag{9}$$

we have

$$\frac{C + k_2 x_1^j}{C + k_3 x_2^j} \leq \frac{C + \varepsilon k_2 x_3^j}{C + k_3(\beta_3 - \varepsilon)x_3^j} \leq \frac{1}{1 + \gamma_3 x_3^j}, \qquad j \geq m_0,$$

with $\gamma_3 = (k_3(\beta_3 - \varepsilon) - 2\varepsilon k_2)/C$ and ε so small that $\gamma_3 > 0$. Then

$$\frac{x_2^m}{x_3^m} = \left(\prod_{j=j_0}^{m-1}\frac{C + k_2 x_1^j}{C + k_3 x_2^j}\right)\frac{x_2^{j_0}}{x_3^{j_0}} = \left(\exp\sum_{j=j_0}^{m-1}\log\frac{C + k_3 x_2^j}{C + k_3 x_2^j}\right)\frac{x_2^{j_0}}{x_3^{j_0}}. \tag{10}$$

Assume j_0 is big enough so that $\gamma_3 x_3^{j_0} < 1$. Using that $\log\frac{1}{1+t} < -(\log 2)t$ for $t \in (0,1)$ we have $\log\frac{C+k_2 x_1^j}{C+k_2 x_2^j} \leq \log\frac{1}{1+\gamma_3 x_3^j} < -(\log 2)\gamma_3 x_3^j$. Taking into account (8) we get that the sum in (10) diverges to $-\infty$ when $m \to \infty$ and hence $\frac{x_2^m}{x_3^m} \to 0$ which is a contradiction.

□

To estimate the distance from $F^m(x^0)$ to $q^{4,4}$ we write

$$\begin{aligned}\|(x_1^m,x_2^m,x_3^m,x_4^m)-(0,0,0,1)\|^2 &= (x_1^m)^2+(x_2^m)^2+(x_3^m)^2+(x_1^m+x_2^m+x_3^m)^2\\ &= 2(x_3^m)^2\left[1+\frac{x_1^m}{x_3^m}+\frac{x_2^m}{x_3^m}+\frac{x_1^m}{x_3^m}\frac{x_2^m}{x_3^m}+\left(\frac{x_1^m}{x_3^m}\right)^2+\left(\frac{x_2^m}{x_3^m}\right)^2\right]\end{aligned} \tag{11}$$

so that the asymptotic behaviour depends on how $\{x_3^m\}$ tends to 0.

Claim 6. *Given $\varepsilon>0$ there exists $m_0\geq 1$ such that*

$$\frac{x_3^{m_0}}{1+(m-m_0)((k_4+\varepsilon\,\nu_2)/C)x_3^{m^0}}\leq x_3^m\leq\frac{x_3^{m_0}}{1+(m-m_0)((k_4+\varepsilon\,\nu_1)/C)x_3^{m^0}},\qquad m\geq m_0, \tag{12}$$

where $\nu_1=k_1-2k_3-k_4$ and $\nu_2=k_3+\varepsilon k_2$.

Proof. By the previous claims we have that $x_1^m<\varepsilon x_3^m$ and $x_2^m<\varepsilon x_3^m$ for $m\geq m_0$. Also $x_1^m,x_2^m,x_3^m<\varepsilon$ for $m\geq m_0$. First we establish the bounds

$$\phi(x^m)\geq\varepsilon k_1x_3^m+k_4(1-\varepsilon)x_3^m,\qquad m\geq m_0,$$

and

$$\phi(x^m)\leq\varepsilon^2k_2x_3^m+\varepsilon\,k_3x_3^m+k_4x_3^m,\qquad m\geq m_0.$$

Then, using (9),

$$\frac{C+k_3x_2^m}{C+\phi(x^m)}\leq\frac{C+\varepsilon k_3x_3^m}{C+(k_4+\varepsilon(k_1-k_4))x_3^m}\leq\frac{1}{1+((k_4+\varepsilon\nu_1)/C)x_3^m}$$

which gives

$$x_3^{m+1}\leq\frac{1}{1+((k_4+\varepsilon\nu_1)/C)x_3^m}x_3^m,$$

and by Lemma 3, we obtain the right hand side inequality of the claim. On the other hand

$$\frac{C+k_3x_2^m}{C+\phi(x^m)}\geq\frac{C}{C+(k_4+\varepsilon(k_3+\varepsilon k_2))x_3^m}=\frac{1}{1+((k_4+\varepsilon\nu_2)/C)x_3^m},$$

and, using Lemma 3 again, we obtain the other inequality. □

With the information on the rate of convergence of $\{x_3^m\}$ we can now estimate, given $x^0\in S^{n-1}\setminus\partial S^{n-1}$, the number of iterations m for $F^m(x^0)$ to arrive to a distance δ from $q^{4,4}$. The condition for m is obtained putting $x_3^m=\delta$ in (12). From this we get

$$\frac{C}{k_4+\varepsilon\nu_2}(1/\delta-1/x_3^{m_0})+m_0<m<\frac{C}{k_4+\varepsilon\nu_1}(1/\delta-1/x_3^{m_0})+m_0.$$

That is, apart from a transitory, the number of iterations for x_3^m to get δ is essentially proportional to C/k_4, and by (11), the number of iterations for x^m to arrive to a neighbourhood of $q^{4,4}$ of radius δ is given by the previous formula changing δ by $\delta/\sqrt{2}$.

5. *Convergence to $q^{3,3}$ (when $k_1\leq 0$).*

Following the same scheme as before, to estimate the distance from $F^m(x^0)$ to $q^{3,3}$ we write

$$\|(x_1^m,x_2^m,x_3^m)-(0,0,1)\|^2=(x_1^m)^2+(x_2^m)^2+(x_1^m+x_2^m)^2=2(x_2^m)^2\left[1+\frac{x_1^m}{x_2^m}+\left(\frac{x_1^m}{x_2^m}\right)^2\right]$$

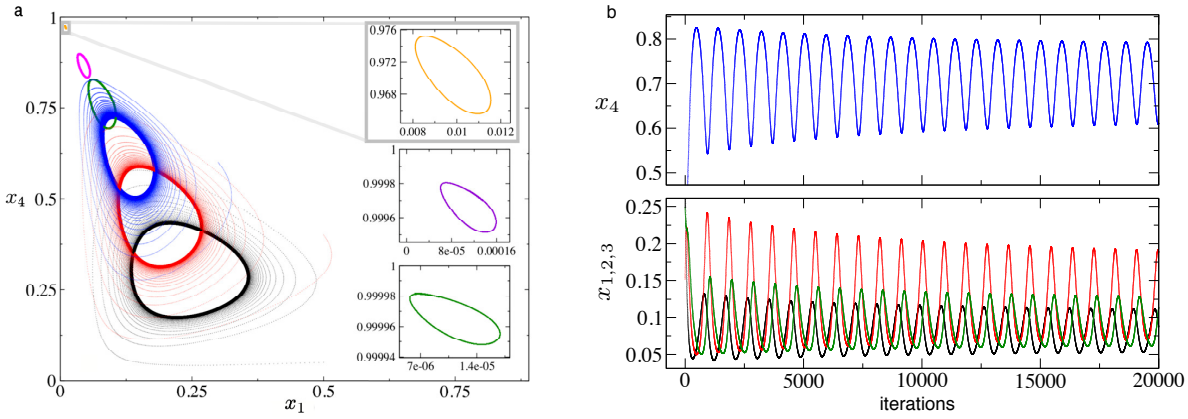

FIG. 6. (a) Evolution of the invariant curve in a projection of the phase space (x_1, x_4) as $k_1 \to 0$ using: $k_1 = 0.8$ (black); $k_1 = 0.4$ (red); $k_1 = 0.2$ (blue); $k_1 = 0.1$ (green); $k_1 = 0.05$ (magenta); and $k_1 = 0.01$ (orange). Insets: (orange) $k_1 = 0.01$; (violet) $k_1 = 10^{-4}$; and (green) $k_1 = 10^{-5}$. Here we have set $k_{2,3,4} = 1$. (b) Time series on the attractor for x_4 (blue) and x_1 (black), x_2 (red), x_3 (green), with $k_1 = 0.1, k_2 = 0.9, k_3 = 0.6$, and $k_4 = 0.8$. In all panels we used $C = 10$.

so that the asymptotic behaviour depends on how $\{x_2^m\}$ tends to 0. We first prove, as in the previous case, that $\{x_1^m/x_2^m\}$ converges to 0. Next we prove that

$$\frac{1}{1+((k_3+\varepsilon\nu_4)/C))x_2^j} \leq \frac{1+k_2x_1^m}{C+\phi(x_2^m)} \leq \frac{1}{C+((k_3+\varepsilon\nu_3)/C))x_2^m}$$

for $m \geq m_0$, with $\nu_3 = k_1 - 2k_2 - k_3$ and $\nu_4 = k_2$. We then check that the number m of iterations to converge from x^0 to a ball of radius δ centered at $q^{3,3}$ satisfies

$$\frac{C}{k_3+\varepsilon\nu_4}(\sqrt{2}/\delta - 1/x_2^{m_0}) + m_0 < m < \frac{C}{k_3+\varepsilon\nu_3}(\sqrt{2}/\delta - 1/x_2^{m_0}) + m_0.$$

6. *Convergence to $q^{2,2}$ (when $k_1 = 0$).*

This case is very particular since the map is one dimensional. Written in terms of x_1 it has the form

$$x_1^{m+1} = \frac{C}{C+k_2x_1^m(1-x_1^m)}x_1^m.$$

For $m \geq m_0$ we have

$$\frac{1}{1+(k_2/C)x_1^m}x_1^m \leq x_1^{m+1} \leq \frac{1}{1+(k_2(1-\varepsilon)/C)x_1^m}x_1^m.$$

Arguing in a similar way, the number of iterations satisfies

$$\frac{C}{k_2}(\sqrt{2}/\delta - 1/x_1^{m_0}) + m_0 < m < \frac{C}{k_2-\varepsilon}(\sqrt{2}/\delta - 1/x_1^{m_0}) + m_0.$$

E. Invariant curve and study of bifurcations for $n = 4$

As previously mentioned and, as a difference from time-continuous models (where oscillations appear for $n \geq 5$ [43, 44, 54]), the dynamics of the map F defined in (1) for $n = 4$ and $k_i > 0$ $(i = 1, ..., 4)$ is governed by an invariant curve [55, 56]. The bifurcation diagrams in Fig. 4 display how the local maxima and minima of all the variables, obtained from time series once the invariant curve has been reached, change at decreasing k_1. For $0 < k_1 \leq 1$ the dynamics is governed by self-sustained, periodic oscillations (see also Fig. 6). Figure 4 also displays how the invariant curve changes within the range $0 < k_1 \leq 1$. The invariant curve shrinks to $q^{4,4} = (0, 0, 0, 1)$ as $k_1 \to 0$. This change

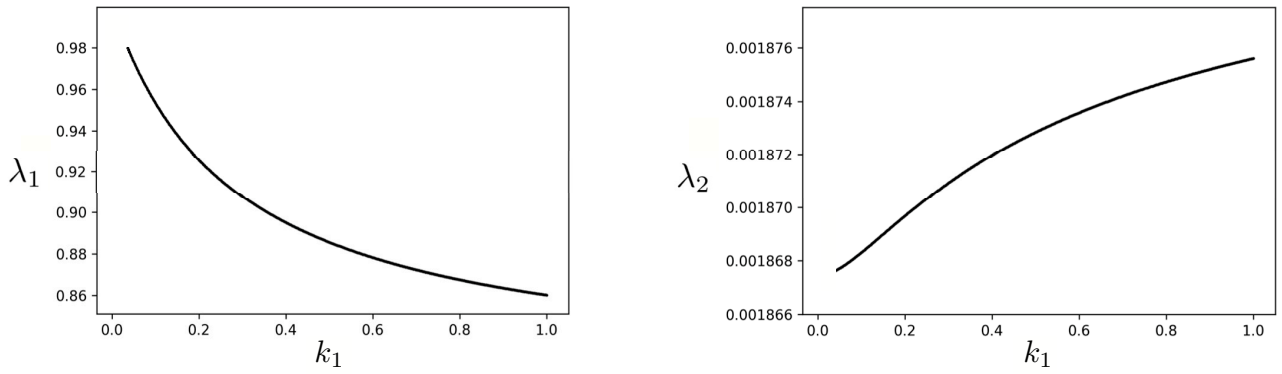

FIG. 7. The two eigenvalues, $\lambda_{1,2}$, of the fixed point resulting from the study of the invariant curve on a Poincaré-like section for the case $n = 4$ (see Section III E). Note that the two eigenvalues are smaller than one within the range $0 < k_1 \leq 1$, indicating that the invariant curve is stable.

in the size of the invariant curve can be visualised in Fig. 6(a), where projections of the attractor in the phase space (x_1, x_4) are shown for decreasing values of k_1. Note that the invariant curve changes in size until it collapses at $k_1 = 0$ (see also Fig. 4). Figure 6(b) displays time series setting $k_1 = 0.1, k_2 = 0.9, k_3 = 0.6$, and $k_4 = 0.8$.

So far, the invariant curve when $n = 4$, described in Ref. [55], was obtained by numerical iteration. Also, the emergence of periodic oscillations for this hypercycle dimension were provided by the presence of a 'Hopf' bifurcation [56] in the asymptotic limit $C \to \infty$. Nowadays many authors call Neimark-Sacker to the bifurcation of families of maps analogous to the Hopf bifurcation for differential equations. The collapse of the invariant curve at $k_1 = 0$ is through a degenerate transcritical-Neimark-Sacker bifurcation different from the one found in [56] when $C \to \infty$. There are several methods to look for invariant curves (and invariant tori). See [14–17] for description and history of these methods. They are based either on conjugating the map to a rotation (parameterization method), on studying the iterations that fall in a thin region (slices method) or interpolating the map in some way. Our results have been obtained using a method based on interpolation similar, but simpler, to the one proposed in [11]. A further elaboration in a much more sophisticated way is found in [59].

To compute the invariant curve we choose a suitable transversal section M (depending on the parameters) close to the expected invariant curve. We choose it as a hyperplane (intersected with S^3) determined by the first variable x_1 fixed at $x_1 = x_1^h$. Since the invariant curve should be not so far from the inner fixed point p^4, we take x_1^h as the first component of p^4. Since the domain of the map is S^3 we will work with the variables x_2, x_3, the variable x_4 being recovered from $x_1 + x_2 + x_3 + x_4 = 1$. Now, given a point $x^0 \in M$, we iterate it until the iterations cross M in the same sense as x^0 goes to $F(x^0)$. This means the second time they cross M. We consider the previous three iterations before reaching M and the three ones after crossing it. To obtain a point in M we interpolate the six points by a (vector) polyomial $p(t) = (p_1(t), p_2(t), p_3(t), p_4(t))$, and then look for t^* such that $P_1(t^*) = x_1^h$; solving the equation using Newton's method. Then $p(t^*) \in M$. We call $G : M \to M$ the map that sends x^0 to $p(t^*)$ obtained by the previous procedure. It can be seen as a pseudo Poincaré map. We emphasise that it is a two dimensional map.

Next we look for a fixed point of G by using Newton's method, approximating the derivatives numerically by the central difference quotient. In this way we have an approximation of a point on the invariant curve. Iterating this point we recover it. In our example two iterations are sufficiently close so that the polynomial interpolation gives a good local representation of the curve. Moreover, the derivative of G at the fixed point provides a good estimate of the hyperbolicity of the invariant curve. The corresponding eigenvalues, computed as a function of k_1, are displayed in Fig. 7.

When $k_1 \to 0$, as we have already mentioned, the invariant curve shrinks to $q^{4,4}$ and disappears for $k_1 \leq 0$ in a Neimark-Sacker bifurcation. At the same time p^4 collides with $q^{4,4}$ undergoing a transcritical bifurcation. All eigenvalues of $DF(q^{4,4})$ are 1 except $1 + k_1/C$ which passes from bigger to less than 1 when k_1 decreases. As for p^4, for $k_1 > 0$, $DF(p^4)$ has two eigenvalues bigger than 1 and one less than 1. For $k_1 < 0$, all its eigenvalues are bigger than 1 (note that in this case p^4 no longer belongs to S^{n-1}). Also, $q^{4,4}$ belongs to the line of fixed points $\{(0, \alpha, 0, 1-\alpha) \mid, \alpha \in \mathbb{R}\}$. Moreover, just at the bifurcation ($k_1 = 0$) a new line of fixed points $\{(\alpha, 0, 0, 1-\alpha) \mid, \alpha \in \mathbb{R}\}$ containing $q^{4,4}$ appears, making the bifurcation even more degenerate.

IV. CONCLUSIONS

Hypercycles have been a subject of intensive research within the last 40 years. This theory has become of paramount importance since it suggests a plausible path towards the origins of life from biochemical self-organisation [1–3, 5]. One of the most important properties of hypercycles is their potential to overcome the so-called error threshold, suggested to be a major constraint in the increase of complexity of the first self-replicating systems in prebiotic ages [1–3]. The hypercycle may allow the stable coexistence of all its members, and thus larger information contents could be stored, as a difference from self-replicating, non-cooperative systems, in which the survival of the fittest may limit species' coexistence and thus genetic diversity [1, 2, 4].

It has been suggested that catalytic RNAs (i.e., ribozymes) could have been the first self-replicating systems in prebiotic evolution [30–33]. RNAs are good candidates since this macromolecules are known to have catalytic activities [26–28, 35–40] as well as the capacity of genetic information storage. The dynamics and stability of catalytic networks is largely determined by its graph structure [4]. For example, several works have investigated the impact of catalytic parasites (i.e., replicators receiving catalytic aid but not providing catalysis to the next members of the cycle) in hypercycles persistence [47–49, 52]. Also, the so-called catalytic short-circuits [50, 51], although less explored, have been studied to determine its impact on hypercycles' persistence. In this contribution, we have analysed a different scenario in which a functional shift in a given species changes the cooperative interaction to an antagonistic one. Specifically, we have studied small hypercycles in which a heterocatalytic interaction shifts to a density-dependent degradation (trans-cleaving activity). Several experimental studies have described trans-cleaving activities in ribozymes [39, 57, 58].

Despite hypercycle dynamics have been widely investigated, most of the research has been performed using time-continuous approaches [1, 43–46, 48, 51, 52]. Only few discrete-time hypercycle systems have been explored [55, 56]. We here have considered that discrete-time hypercycle introduced by Hofbauer [55]. However, here, in contrast with [55], we have investigated how functional shifts impact the dynamics of small hypercycles with $n = 2, 3, 4$ species. Fixed points and stability analyses are developed for these systems. In this discrete-time setting, hypercycles with $n = 4$ display an oscillatory state allowing the coexistence of all the species via an invariant curve, while smaller hypercycles achieve coexistence via an interior fixed point. We provide a proof for the $\omega-$limit of hypercycles when one replicator undergoes directed degradation, shown to be given by the out-competition of all the cooperative species by the one conducting the degradation. This functional change from cooperation to directed degradation makes the hypercycle become more similar to a catalytic chain. Our results are in agreement with previous research describing the impossibility of replicators' coexistence in linear catalytic chains [4].

The convergence times to the fixed points have been analytically obtained and the relevant parameters in the asymptotic expressions identified. Concretely, we have obtained that for the points p^n, $n = 2, 3$, the times are proportional to $C(\sum_{i=1}^{n} \frac{1}{k_i})$, $n = 2, 3$, and for the points $q^{n,n}$, $n = 2, 3, 4$, the times are proportional to C/k_n. Numerical computations confirm the results and illustrate the behaviour. We have also described the bifurcations tied to the functional shift in one of the replicators. For cases $n = 2, 3$ a transcritical bifurcation is responsible for the extinction of the hypercycle. When $n = 4$, the analytical/numerical computations lead us to conclude there is a degenerate transcritical–Neimark-Sacker bifurcation when $k_1 \to 0$ as described at the end of Section III E. We emphasize that this bifurcation is different from the one described in [56] that occurs when $C \to \infty$.

As mentioned in the Introduction, hypercycle equations have been used to model the dynamics of different nonlinear systems such as cooperativity in ecosystems [5, 18], virus replication [8–10, 12], and, more recently, experimentally-built synthetic systems using bacteria [22] and yeast [21]. We want to notice that our contribution, albeit carrying a deep mathematical background, aims to model the changes introduced by functional shifts that can occur in molecular replicators by mutation processes. Indeed, functional shifts are found in ecological systems and are usually caused by behavioural or environmental changes. We are here focusing on changes in ribozymes switching their phenotype from the cooperative to the degradative one (self-cleaving). In terms of complex ecosystems, such functional shifts can be given by transitions between cooperation and competition. These shifts have been described in plants in semiarid ecosystems (the so-called stress-gradient hypothesis), in which facilitation (cooperation) increase as resources (e.g., water availability) decrease [62].

ACKNOWLEDGMENTS

This work has been partially funded by the "Mar´ia de Maeztu" Programme for Units of Excellence in R&D (MDM-2014-0445) and by the CERCA Programme of the Generalitat de Catalunya. JS has been funded by a "Ramón y Cajal" contract (RYC-2017- 22243) and by the Spain's "Agencia Estatal de Investigación" grant RTI2018-098322-B-I00. The research leading to these results has been also funded by "la Caixa" Foundation. EF has been supported by

grants MTM2016-80117-P (MINECO/FEDER, UE) and 2017-SGR-1374 (Catalan Autonomous Government).

[1] M. Eigen, P. Schuster, The Hypercycle. A Principle of Natural Self-Organization. Springer-Verlag, Berlin, 1979.
[2] M. Eigen, Selforganization of matter and the evolution of biological macromolecules, Naturwiss. 58(10) (1971) 465-523.
[3] S.A. Kauffman, The origins of order: self-organization and selection in Evolution, Oxford University Press, Inc. 1993.
[4] B. Stadler, P. Stadler, Molecular Replicator Dynamics, Adv. Complex Syst. 6(01) (2003) 47-77.
[5] J.M. Smith, E. Szathmáry, The major transitions in evolution, Oxford University Press, 1995.
[6] M.A. Cohen, S. Grossberg, Absolute stability and global pattern formation and parallel memory storage by competitive neural networks, IEEE Trans Syst Man Cybernet 13 (1983) 815-826.
[7] M.A. Cohen, S. Grossberg, Pattern recognition by self-organizing neural networks, MIT Press, Cambridge, MA, 1991.
[8] E. Szathmáry, Natural selection and dynamical coexistence of defective and complementing virus segments, J. Theor. Biol. 157 (1992) 383-406.
[9] E. Szathmáry, Co-operation and defection: playing the field in virus dynamics, J. Theor. Biol. 165 (1993) 341-356.
[10] J. Sardanyés, S.F. Elena, Error threshold in RNA quasispecies models with complementation, J. Theor. Biol. 265 (2010) 278-286.
[11] C. Simó, Effective computations in celestial mechanics and astrodynamics in Modern methods of analytical mechanics and their applications (Udine, 1997), 55–102, CISM Courses and Lect., 387, Springer, Vienna, 1998.
[12] M. Eigen, C.K. Biebricher, M. Gebinoga, The Hypercycle. Coupling of RNA and Protein Biosynthesis in the Infection Cycle of an RNA Bacteriophage, Biochem. 30 (1991) 11005-11018.
[13] J.D. Farmer, S.A. Kauffman, N.H. Packard, A.S. Perelson, Adaptive dynamic networks as models for the immune system and autocatalytic sets, in: Perspectives in biological dynamics and theoretical medicine, Annals of the New York Academy of Sciences, 1987.
[14] À. Haro, M. Canadell, J.L. Figueras, A. Luque, J.M. Mondelo, The parameterization method for invariant manifolds. From rigorous results to effective computations. Applied Mathematical Sciences, 195. Springer, 2016.
[15] À. Haro, R. de la Llave, A parameterization method for the computation of invariant tori and their whiskers in quasi-periodic maps: rigorous results. J. Differential Equations 228(2) (2006), 530–579.
[16] Schilder, Frank; Osinga, Hinke M.; Vogt, Werner Continuation of quasi-periodic invariant tori. SIAM J. Appl. Dyn. Syst. 4(3) (2005), 459–488.
[17] C. Froeschlé, Numerical study of dynamical systems with three degrees of freedom. I. Graphical displays of four-dimensional sections. Astronom. and Astrophys. 4 (1970) 115–128.
[18] J. Sardanyés, The Hypercycle: from molecular to ecosystems dynamics, in: Landscape ecology research trend, Nova Publishers, 2009.
[19] M.A. Nowak, D.C. Krakauer, The evolution of language, Proc. Natl. Acad. Sci. U.S.A. 96(14) (1999) 8028-8033.
[20] D.H. Lee, K. Severin, Y. Yokobayashi, M.R. Ghadiri, Emergence of symbiosis in peptide self-replication through a hypercyclic network, Nature 390 (1997) 591-594.
[21] W. Shou, S. Ram, J.M.G. Vilar, Synthetic cooperation in engineered yeast populations, Proc. Natl. Acad. Sci. U.S.A. 104(6) (2007) 1877-1882.
[22] D.R. Amor, R. Montañez, S. Duran-Nebreda, R.V. Solé, Spatial dynamics of synthetic microbial mutualists and their parasites, PLoS Comput. Biol. 13(8) (2017), e15689.
[23] U. Niesert, D. Harnasch, C. Bresch, Origin of life between scylla and charybdis, J. Mol. Evol. 17 (1981) 348-353.
[24] D.A. Usher, A.H. McHale, Hydrolyitc stability of helical RNA: A selective advantage for the natural $3', 5'-$ bond, Proc. Natl. Acad. Sci. U.S.A. 73(4) (1976) 1149-1153.
[25] R. Lohrmann, L.E. Orgel, Self-condensation of activated dinucleotides on polynucleotide templates with alternating sequences, J. Mol. Evol. 14 (1979) 243-250.
[26] T.R. Cech, The chemistry of self-replicating RNA and RNA enzymes, Science 236 (1987) 1532-1539.
[27] J.A. Daròs, Eggplant latent viroid: a friendly experimental system in the family Asunviroidae, Mol. Plant Pathol. 17 (2016) 1170-1177.
[28] R.M. Jimenez, J.A. Polanco, A. Lupták, Chemistry and biology of self-cleaving ribozymes, Trends Biochem. Sci. 40(11) (2015) 648-661.
[29] K. Kruger, P.J. Grabowski, A.J. Zaug, J. Sands, D.E. Gottschling, T.R. Cech, Self-splicing RNA: autoexcision and autocyclization of the ribosomal RNA intervening sequence of Tetrahymena, Cell 31(1) (1982) 147-157.
[30] M. Neveu, H.J. Kim, S.A. Benner, The "strong" RNA world hypothesis: fifty years old, Astrobiology. 13(4) (2013) 391-403.
[31] J. A. Doudna, T.R. Cech, The chemical repertoire of natural ribozymes, Nature 418 (2002) 222-228.
[32] M.P. Robertson, G.F. Joyce, The origins of the RNA world, Cold Spring Harbor Perspectives in Biology. 4(5) (2012) a003608.
[33] A.V. Vlassov, Mini-ribozymes and freezing environment: a new scenario for the early RNA world, Biogeosci. Discuss. 2 (2005) 1719-1737.
[34] F.H.C. Crick, A speculation on the origin of protein synthesis, Orig. Life 7(4) (1976) 389-397.
[35] B. Zhang, T.R. Cech, Peptidyl-transferase ribozymes: trans reactions, structural characterization and ribosomal RNA-like features, Chem Biol. 5(10) (1998) 539-53.

[36] M.D. Been, E.T. Barford, J.M. Burke, J.V. Price, N.K. Tanner, A.J. Zaug, T.R. Cech, Structures involved in Tetrahymena rRNA self-splicing and RNA enzyme activity, Cold Spring Harb. Symp. Quant. Biol. 52 (1987) 147-157.

[37] W.S. Zielinksi, L.E. Orgel, Oligomerization of activated derivatives of 3′−amino−3′−deoxyguanosine on poly(C) and poly(dC) template, Nucl. Acid Res. 13(24), (1985) 8999-9009.

[38] G. Von Kiedrowski, A self-replicating hexadeoxynucleotide, Angew. Chem. Int. Ed. 119(10) (1986) 932-935.

[39] A. Carbonell, R. Flores, S. Gago, Trans-cleaving hammerhead ribozymes with tertiary stabilizing motifs: in vitro and in vivo activity against a structured viroid RNA, Nucl. Acid Res. 39(6) (2011) 2432-2444.

[40] C.E. Weinberg, Z. Weinberg, C. Hammann, Noverl ribozymes: discovery, catalytic mechanisms, and the quest to understand biological functions, Nucl. Acid Res. 47(18) (2019) 9480-9494.

[41] C.E. Weinberg, Z. Weinberg, C. Hammann, In-ice evolution of RNA polymerase ribozyme activity, Nature Chem. 5(12) (2013) 1011-1018.

[42] N. Vaidya, M.L. Manapat, I.A. Chen, R. Xulvi-Brunet, E.J. Hayden, N. Lehman, Spontaneous network formation among cooperative RNA replicators, Nature 491(18) (2012) 72-77.

[43] D.A.M.M. Silvestre, J.F. Fontanari, The information capacity of hypercycles, J. Theor. Biol. 254(4) (2008) 804-806.

[44] A. Guillamon, E. Fontich, J. Sardanyés, Bifurcations analysis of oscillating hypercycles, J. Theor. Biol. 387 (2015) 23-30.

[45] G. Farré, J. Sardanyés, A. Guillamon, E. Fontich, Coexistence stability in a four-member hypercycle with error tail through center manifold analysis, Nonlinear Dyn. 90 (2017) 1873-1883.

[46] J Sardanyés, R.V. Solé, Bifurcations and phase transitions in spatially extended two-member hypercycles, J. Theor. Biol. 243 (2006) 468-482.

[47] M.C. Boerlijst, P. Hogeweg, Spiral wave structure in prebiotic evolution: Hypercycles stable against parasites, Physica D 48 (1991) 17-28.

[48] J. Sardanyés, R.V. Solé, Spatio-temporal dynamics in simple asymmetric hypercycles under weak parasitic coupling, Physica D 231 (2007) 116-129.

[49] M.C. Boerlijst, P. Hogeweg, Spatial gradients enhance persistence of hypercycles, Physica D 88 (1995) 29-39.

[50] J. Sardanyés, J.T. Lázaro, A. Guillamon, E. Fontich. Full analysis of small hypercycles with short-circuits in prebiotic evolution, Physica D 34 (2017) 90-108.

[51] P.J. Kim, H. Jeong, Spatio-temporal dynamics in the origin of genetic information, Physica D 203 (2005) 88-99.

[52] M.B. Cronhjort, Cluster compartmentalization may provide resistance to parasites for catalytic networks, Physica D 101 (1997) 289-298.

[53] J. Sardanyés, R.V. Solé, Delayed transitions in non-linear replicator networks: About ghosts and hypercycles, Chaos, Solitons & Fractals 31 (2007) 305-315.

[54] J. Hofbauer, J. Mallet-Paret, H. L. Smith, Stable periodic solutions for the hypercycle system. J. Dyn. Diff. Eq. 3(3) (1995) 423-436.

[55] J. Hofbauer, A Difference Equation Model for the Hypercycle, SIAM J. Appl. Math. 44 (1984) 762-772.

[56] J. Hofbauer, G. Iooss, A Hopf Bifurcation Theorem for Difference Equations. Approximating a Differential Equation, Monatsh. Math. 98 (1984) 99-113.

[57] O.C. Uhlenbeck, A small catalytic oligoribonucleotide, Nature 328 (1987) 596-600.

[58] J. Haseloff, W.L. Gerlach, Simple RNA enzymes with new and highly specific endoribonuclease activities, Nature 334 (1988) 585-591.

[59] V. Gelfreich, A. Vieiro, Interpolating vector fields for near identity maps and averaging, Nonlinearity 31(9) (2018) 4263-4289.

[60] R. M. Gray, Toeplitz and Circulant Matrices: A Review, Foundations and Trends in: Communications and Information Theory 2(3) (2006) 155-239.

[61] V.I. Arnol'd, Geometrical methods in the theory of ordinary differential equations, Springer-Verlag, New York-Berlin, 1983.

[62] M.J. O'Brien, F.J. Pugnaire, C. Armas, S. Rodriguez-Echeverria, C. Schöb, The shift from plant-plant facilitation to competition under severe water deficit is spatially explicit. Ecol Evol 31(9) (2018) 4263-4289.